Quantitative biokinetics of titanium dioxide nanoparticles after oral administration in rats (Part 2)

Journal:	*Nanotoxicology*
Manuscript ID	TNAN-2016-0177.R2
Manuscript Type:	Original Article
Date Submitted by the Author:	n/a
Complete List of Authors:	Kreyling, Wolfgang; Helmholtz Center Munich – German Research Center for Environmental Health, Comprehensive Pneumology Center, Institute of Lung Biology and Disease; Helmholtz Center Munich – German Research Center for Environmental Health, Institute of Epidemiology 2 Holzwarth, Uwe; Joint Research Centre, Institute for Health and Consumer Protection Schleh, Carsten; Helmholtz Center Munich – German Research Center for Environmental Health, Comprehensive Pneumology Center, Institute of Lung Biology and Disease Kozempel, Ján; Joint Research Centre, Institute for Health and Consumer Protection Wenk, Alexander; Helmholtz Center Munich – German Research Center for Environmental Health, Comprehensive Pneumology Center, Institute of Lung Biology and Disease Haberl, Nadine; Helmholtz Center Munich – German Research Center for Environmental Health , Comprehensive Pneumology Center, Institute of Lung Biology and Disease Hirn, Stephanie; Helmholtz Zentrum München – German Research Center for Environmental Health, Comprehensive Pneumology Center, Institute of Lung Biology and Disease Schäffler, Martin; Helmholtz Center Munich – German Research Center for Environmental Health, Comprehensive Pneumology Center, Institute of Lung Biology and Disease Lipka, Jens; Helmholtz Zentrum Munchen Deutsches Forschungszentrum fur Umwelt und Gesundheit, Comprehensive Pneumology Center, Institute of Lung Biology and Disease

	Semmler-Behnke, Manuela; Helmholtz Zentrum München – German Research Center for Environmental Health, Comprehensive Pneumology Center, Institute of Lung Biology and Disease Gibson, Neil; Joint Research Centre, Institute for Health and Consumer Protection
Keywords:	Size-selected, radiolabeled titanium dioxide nanoparticles, gavage, gut-absorption, accumulation in secondary organs and tissues, different biokinetics pattern after gavage versus intravenous injection
Abstract:	The biokinetics of a size-selected fraction (70nm median size) of commercially available and 48V-radiolabeled [48V]TiO2 nanoparticles has been investigated in female Wistar-Kyoto rats at retention timepoints 1h, 4h, 24h and 7days after oral application of a single dose of an aqueous [48V]TiO2-nanoparticle suspension by intra-esophageal instillation. A completely balanced quantitative body clearance and biokinetics in all organs and tissues was obtained by applying typical [48V]TiO2-nanoparticle doses in the range of 30–80 μg•kg-1 bodyweight, making use of the high sensitivity of the radiotracer technique. The [48V]TiO2-nanoparticle content was corrected for nanoparticles in the residual blood retained in organs and tissue after exsanguination and for 48V-ions not bound to TiO2-nanoparticles. Beyond predominant fecal excretion about 0.6% of the administered dose passed the gastro-intestinal-barrier after -h and about 0.05% were still distributed in the body at day-7, with quantifiable [48V]TiO2-nanoparticle organ concentrations present in liver (0.09ng•g-1), lungs (0.10ng•g-1), kidneys (0.29ng•g-1), brain (0.36ng•g-1), spleen (0.45ng•g-1), uterus (0.55ng•g-1) and skeleton (0.98ng•g-1). Since chronic, oral uptake of TiO2 particles (including a nano-fraction) by consumers has continuously increased in the past decades , the possibility of chronic accumulation of such biopersistent nanoparticles in secondary organs and the skeleton raises questions about the responsiveness of their defense capacities, and whether these could be leading to adverse health effects in the population at large. After normalizing the fractions of retained [48V]TiO2-nanoparticles to the fraction that passed the gastro-intestinal-barrier and reached systemic circulation the biokinetics was compared to the biokinetics determined after IV-injection (Part 1). Since the biokinetics patterns differ largely IV-injection is not an adequate surrogate for assessing the biokinetics after oral exposure to TiO2 nanoparticles.

Quantitative biokinetics of titanium dioxide nanoparticles after oral application in rats (Part 2)

Wolfgang G. Kreyling*#§, Uwe Holzwarth+, Carsten Schleh*[1], Ján Kozempel+[2], Alexander Wenk*[3], Nadine Haberl*, Stephanie Hirn*, Martin Schäffler*, Jens Lipka*, Manuela Semmler-Behnke*[4], Neil Gibson+.

* Helmholtz Zentrum München – German Research Center for Environmental Health, Comprehensive Pneumology Center, Institute of Lung Biology and Disease, Ingolstaedter Landstrasse 1, D-85764 Neuherberg / Munich, Germany

Helmholtz Center Munich – German Research Center for Environmental Health, Institute of Epidemiology 2, Ingolstaedter Landstrasse 1, D-85764 Neuherberg / Munich, Germany

+European Commission, Joint Research Centre, Directorate F – Health, Consumers and Reference Materials, Via E. Fermi 2749, I-21027 Ispra (VA), Italy

§Corresponding author:

Dr. Wolfgang G. Kreyling

Institute of Epidemiology 2

Helmholtz Centre Munich, German Research Center for Environmental Health

D-85764 Neuherberg / Munich

Germany

Email: kreyling@helmholtz-muenchen.de

Phone: +49-89-2351-4817

KEYWORDS

[1] Current address: Abteilung Gesundheitsschutz, Berufsgenossenschaft Holz und Metall, D-81241 München, Germany

[2] Current address: Czech Technical University in Prague, Faculty of Nuclear Sciences and Physical Engineering, Břehová 7, CZ-11519 Prague 1, Czech Republic

[3] Current address: Dept. Infrastructure, Safety, Occupational Protection, German Research Center for Environmental Health, D-85764 Neuherberg / Munich, Germany

[4] Current address: Bavarian Health and Food Safety Authority, D-85764 Oberschleissheim, Germany

Size-selected, radiolabeled titanium dioxide nanoparticles; gavage; gut-absorption; accumulation in secondary organs and tissues; different biokinetics pattern after gavage versus intravenous injection

ABSTRACT

The biokinetics of a size-selected fraction (70nm median size) of commercially available and ^{48}V-radiolabeled [^{48}V]TiO_2 nanoparticles has been investigated in female Wistar-Kyoto rats at retention timepoints 1h, 4h, 24h and 7days after oral application of a single dose of an aqueous [^{48}V]TiO_2-nanoparticle suspension by intra-esophageal instillation. A completely balanced quantitative body clearance and biokinetics in all organs and tissues was obtained by applying typical [^{48}V]TiO_2-nanoparticle doses in the range of 30–80 $\mu g \cdot kg^{-1}$ bodyweight, making use of the high sensitivity of the radiotracer technique.

The [^{48}V]TiO_2-nanoparticle content was corrected for nanoparticles in the residual blood retained in organs and tissue after exsanguination and for ^{48}V-ions not bound to TiO_2-nanoparticles. Beyond predominant fecal excretion about 0.6% of the administered dose passed the gastro-intestinal-barrier after -h and about 0.05% were still distributed in the body at day-7, with quantifiable [^{48}V]TiO_2-nanoparticle organ concentrations present in liver ($0.09 ng \cdot g^{-1}$), lungs ($0.10 ng \cdot g^{-1}$), kidneys ($0.29 ng \cdot g^{-1}$), brain ($0.36 ng \cdot g^{-1}$), spleen ($0.45 ng \cdot g^{-1}$), uterus ($0.55 ng \cdot g^{-1}$) and skeleton ($0.98 ng \cdot g^{-1}$). Since chronic, oral uptake of TiO_2 particles (including a nano-fraction) by consumers has continuously increased in the past decades , the possibility of chronic accumulation of such biopersistent nanoparticles in secondary organs and the skeleton raises questions about the responsiveness of their defense capacities, and whether these could be leading to adverse health effects in the population at large.

After normalizing the fractions of retained [^{48}V]TiO_2-nanoparticles to the fraction that passed the gastro-intestinal-barrier and reached systemic circulation the biokinetics was compared to the biokinetics determined after IV-injection (Part 1). Since the biokinetics patterns differ largely IV-injection is not an adequate surrogate for assessing the biokinetics after oral exposure to TiO_2 nanoparticles.

Introduction

On a daily basis, a typical individual in the Western world ingests an estimated average of 2.5 mg of insoluble, submicrometer titanium dioxide (TiO_2) particles, including a nanoparticulate fraction, equivalent to an estimated 10^{12}-10^{14} particles, while the most elevated levels may be as high as 112 mg•d^{-1} (Lomer, 2004), corresponding to an upper dose of 1.6 mg•kg^{-1} body weight.

Major sources of dietary TiO_2 are food additives (E171), confectionary products, pharmaceuticals, cosmetics and health care products such as swallowed toothpaste. Many of these ingested particles are larger than 100 nm diameter. Hence by most current definitions they are not considered as nanoparticles. However, all TiO_2 food additives are characterized by a wide size distribution, and by number, up to 36% of the particles of food grade TiO_2 are nano-sized (Weir, 2012). A recent study supported this finding and revealed that in 27 food products and personal care products 10-25% of the number of TiO_2 particles are below 100 nm in size (Peters, 2014).

A study on seven male subjects using TiO_2 anatase particles with a mean size of 160 nm and 380 nm showed that the particles were partially absorbed by the human gut leading to peak titanium levels in blood between 4 and12 hours post oral ingestion (Bockmann, 2000, Pele, 2015). The insolubility of TiO_2 suggests particle uptake. However, a recent study on 9 volunteers with particles sizes of 15nm, 100nm and <5µm could not find significant evidence for absorption of TiO_2 nanoparticles after oral application (Jones, 2015).

Also studies looking at TiO_2 absorption, retention and toxicity in animal models have led to conflicting results depending on chosen doses, sizes and phase of the TiO_2. Difficulties in quantitative analysis when separating the Ti contribution of nanoparticles from a chemically identical background have very likely contributed to this situation, as illustrated by (MacNicoll, 2015) who found no evidence of a general translocation of TiO_2 nanoparticles after oral application (5mg•kg^{-1} BW) though the authors could not exclude the possibility based on Ti detection in a few individual animals. Another recent study using 'low' doses (2.3 mg) of TiO_2 nanoparticles (various types ranging from 107-360 nm hydrodynamic diameter) in adult healthy rats led to non-significant increases of Ti in liver and spleen but accumulations in mesenteric lymph nodes (Geraets, 2014). An

earlier study of Jani and coworkers found that 12.5 mg/rat of orally administered TiO_2 rutile particles with a mean size of 500 nm could cross the gut walls and accumulate in liver, spleen and lungs (Jani, 1994b) while (Tassinari, 2014) found increased Ti levels in the spleen and ovaries of rats and observed DNA damage following oral application of TiO_2NP doses of 2 mg•kg^{-1} BW (Tassinari, 2014).

A comprehensive review summarizing the current knowledge on toxicokinetics and toxicological responses after application of TiO_2NP by various routes is that of (Shi, 2013). The authors state that there is not much literature available for orally administered TiO_2 nanoparticles.

To estimate the risk associated with dietary TiO_2NP, one has (i) to quantify their uptake following ingestion, (ii) to study their biokinetics and to (iii) identify organs and tissues of concern. To date there are no suitable robust data available. Hence, we aimed here to investigate the biokinetics of orally applied TiO_2 nanoparticles by radiolabeling commercially available TiO_2 anatase nanoparticles with radioactive ^{48}V and selecting a nano-fraction (hydrodynamic diameter 70 nm) which was then applied by intra-esophageal instillation (gavage) to healthy adult female rats. By using γ-ray spectrometry we were able to follow the entire nanoparticle absorption, distribution and excretion for each rat in a fully quantitative manner. Biodistributions of the applied [^{48}V]TiO_2NP were obtained at the time points of 1h, 4h, 24h, and 7d after application, the same retention time points selected for the intravenous injection study (Part 1) in order to catch fast uptake and slower clearance and relocation effects[2].

Materials and Methods

Radiolabeling, suspension preparation and size selection of TiO_2NP

[2] See Materials and Methods where we explain: no further animals were sacrificed for a 28-day biodistribution study after observing in the 7-day experiment that fecal excretion of [^{48}V]TiO_2NP was already complete after 4-5 days.

Two batches of 20 mg ST-01 TiO_2NP were irradiated with a proton beam current of 5 μA and a proton energy of 13.5 MeV. One yielding an activity concentration of 1.0 MBq•mg^{-1} (^{48}V-activity per TiO_2NP mass) was used for the 1h, 4h and 24h retention experiments. The second one was irradiated on five consecutive days, yielded an activity concentration of 2.35 MBq•mg^{-1} and was used for the 7d retention experiment. At these radioactivity concentrations the atomic ratio of ^{48}V:Ti in the NP is about 2.6×10^{-7} and 6.2×10^{-7}, respectively. Since proton irradiation and the chemical difference of the radiolabel may result in a non-perfect integration of the ^{48}V in the TiO_2 matrix, the [^{48}V]TiO_2NP were repeatedly washed to remove released ^{48}V-ions.

Size selection was performed in a repeated sequence of nanoparticle suspension, ultrasound homogenization, washing by centrifugation and re-suspension in distilled water in order to remove excess sodium pyrophosphate, to eliminate larger aggregates/agglomerates and to minimize the content of free, ionic ^{48}V, as described in the Supplementary Information (SI-GAV). The final size-selected and radiolabeled, nano-sized aggregates or agglomerates of [^{48}V]TiO_2NP were suspended in water.

For each of the studied retention time points a new batch of size-selected [^{48}V]TiO_2NP was prepared, characterized and immediately applied in a single dose to four rats for each exposure route, i.e., intravenously, by gavage and intratracheal instillation, which improves the comparability between the exposure routes as the studies were started with the same nanoparticle properties.

Characterization of nanoparticles

The hydrodynamic diameter of the size selected [^{48}V]TiO_2NP and the zeta potential were measured in triplicates several times during the size-selection process for control purposes, and prior to application, using a Malvern Zetasizer (DLS, Malvern, Herrenberg, Germany). Samples for transmission electron microscopy, from the aqueous suspension ready for administration, were prepared on glow discharged Formvar® coated 300mesh copper grids, and investigated with a Philips 300 TEM at 60 kV acceleration voltage.

In order to study the effect of the passage of [^{48}V]TiO_2NP through the gastro-intestinal tract (GIT) [^{48}V]TiO_2NP suspensions were subjected to pH=2 for 30 minutes to simulate the passage through the stomach followed by additional 2 hours at pH=9 to simulate the passage through the small intestine. The evolution of the hydrodynamic diameter was followed by DLS measurements.

Experimental procedures – Study design

It was planned to study the biokinetics of [^{48}V]TiO_2NP with five retention time points 1h, 4h, 24h, 7d and 28d after gavage in four rats for each time point, as for the other exposure routes. However, after observing in the 7-day experiment that fecal excretion of [^{48}V]TiO_2NP was already complete after 4-5 days, no further animals were sacrificed for a 28-day biodistribution study; as sketched below.

Study	Gavage, 0h	dissection time-points for biodistribution analyses			
MAIN-1	[^{48}V]TiO_2NP	1h	4h	24h	7d
MAIN-2	[^{48}V]TiO_2NP	1h	4h	24h	
AUX	^{48}V ions			24h	7d

Immediately after the final preparation step the [^{48}V]TiO_2NP suspensions were applied in a single bolus of about 10µg of [^{48}V]TiO_2NP per rat. The time point at 7d was studied with a higher dose of about 30µg in order to preserve sufficient sensitivity in spite of longer radioactive decay, and to reveal also minor redistribution and clearing processes.

An additional biokinetics study (MAIN-2) was performed in three other groups of four rats each in order to study the amount of [^{48}V]TiO_2NP which remained in the GIT walls, and could possibly reach systemic circulation at later time points. The accumulation of [^{48}V]TiO_2NP was investigated after 1h, 4h, and 24h in the walls and chime (contents) of the stomach and of the small and large intestine.

In order to investigate the absorption and biodistribution of soluble, ionic ^{48}V an AUXiliary study was performed at 24h and 7d after gavage in four rats each with the purpose of correcting the biodistributions of [^{48}V]TiO_2NP for contributions of ^{48}V-ions possibly released from the [^{48}V]TiO_2NP. In order to mimic ^{48}V released by [^{48}V]TiO_2NP 0.33 $\mu g \bullet \mu L^{-1}$ ionic $Ti(NO_3)_4$ was added to carrier-free ionic ^{48}V. The pH value was adjusted to 5. For the experiments 60 µL of solution containing 27 kBq ionic ^{48}V and 20 µg of ionic Ti were administered in each rat. Based on the biodistribution of ^{48}V ions, the urinary excretion kinetics after gavage of ^{48}V-ions and of [^{48}V]TiO_2NP, the biodistribution of [^{48}V]TiO_2NP was corrected for the contribution of ^{48}V-ions according to the mathematical procedure derived in the SI-GAV.

Animals

Healthy, female Wistar-Kyoto rats (Janvier, Le Genest Saint Isle, France), 8–10 weeks of age (263 ± 10 g mean body weight (± STD)) were housed in pairs in relative-humidity and temperature controlled ventilated cages on a 12h day/night cycle. Rodent diet and water were provided ad libitum. After purchase, the rats were adapted for at least two weeks and then randomly attributed to the experimental groups. All experiments were conducted under German federal guidelines for the use and care of laboratory animals and were approved by the Regierung von Oberbayern (Government of District of Upper Bavaria, Approval No. 211-2531-94/04) and by the Institutional Animal Care and Use Committee of Helmholtz Centre Munich.

[^{48}V]TiO_2NP suspensions were applied to non-fasted rats by oral gavage in a single bolus. The rats were first anesthetized by inhalation of 5% isoflurane in oxygen until muscular tonus relaxed, then they were fixed with their incisors to a rubber band on a board at an angle of 60° to the lab bench in a supine position. For intra-esophageal instillation (gavage), a flexible cannula was placed into the upper third of the esophagus and the [^{48}V]TiO_2NP suspension (60 µL) was gently instilled using a 1-mL-insulin-syringe (0.4 µL dead volume) followed by 100 µL of air to accelerate the suspension into the stomach.

After gavage, rats were kept individually in metabolism cages for separate daily collection of urine and feces. At 1h, 4h, 24h and 7d after oral application, rats were anesthetized (by 5% isoflurane inhalation) and euthanized by exsanguination via the abdominal aorta.

Sample preparation and radiometric analysis

After application the syringe and cannula used for gavage were collected for measurements of residual [^{48}V]TiO_2NP retained therein.

For γ-ray spectrometry, all organs, tissues, carcass and excretions were collected and ^{48}V-radioactivities were measured without any further physico-chemical processing (Hirn, 2011, Kreyling, 2011, Kreyling, 2014, Schleh, 2012) to obtain quantitative, fully balanced biodistributions of each rat. Since by exsanguination only about 60-70% of the blood volume could be recovered the residual blood contents of organs and tissues after exsanguination were calculated according to the findings of (Oeff, 1955) and the ^{48}V-activity associated with the residual blood content was subtracted as outlined in SI-GAV.

The radioactivity of the samples was measured by γ-ray spectrometry using shielded NaI detectors properly calibrated in γ-ray energy and detection efficiency for the 511keV radiation produced by decaying ^{48}V. Samples yielding background-corrected counts in the 511eV region-of-interest of the ^{48}V γ-ray spectrum were considered below the detection limit (DL; < 0.2 Bq) when the number of counts was less than three standard deviations of the background counts.

Throughout this report, the determined background and decay corrected ^{48}V-activity values of organs, tissues, blood or excretions are given as percentages of the total applied [^{48}V]TiO_2NP radioactivity, determined as the sum of all samples prepared from each entire animal, including its total fecal and urinary excretions. These percentages are averaged over four rats in each group and are given with the standard error of the mean (SEM). These raw data were corrected (i) for the residual blood content in organs or tissues after exsanguination and (ii) for the activity contribution of free ^{48}V ions according to the methods presented in the SI-GAV.

All calculated significances are based on the One-Way-ANOVA test and the *post hoc* Tukey test. For direct comparisons between two groups, the unpaired t-test was used. $p \leq 0.05$ was considered significant.

Results

Physicochemical properties of [^{48}V]TiO_2NP

The size distributions of the size-selected [^{48}V]TiO_2NP determined by DLS are presented in Figure 1 and indicate a good reproducibility of the size selection procedure. The Z-averages (Table 1) are in a narrow range of 88 ± 11 nm, and the PDI values 0.18 ± 0.04 indicate that the size distributions are polydisperse but with a rather narrow size distribution. TEM investigations after the size selection and dispersion process (Figure 2) revealed approximately spherical aggregated/agglomerated entities of roughly 50 nm in diameter, made up of smaller primary particles.

With the known ^{48}V-activity concentrations (1 MBq•mg^{-1} (1h, 4h, 24h) and 2.35 MBq•mg^{-1} (7d)) of proton irradiated nanoparticles all determined activity values were converted in [^{48}V]TiO_2NP mass. The applied ^{48}V-activities and corresponding masses of [^{48}V]TiO_2NP are reported in Table 1. Since a fraction of the ^{48}V-activity loaded into the syringes was retained there, the effective ^{48}V-activity received by the rats presented in Table 1 specifies the dose effectively received by the rats. It was determined from the activity balance over all organs, tissues, carcass and excretions of each rat. The difference between the activity loaded into the syringes and this effective dose matches the determined retained activity in the application equipment.

The simulation of the GIT passage by exposing the [^{48}V]TiO_2NP suspensions to different pH-values (pH=2 for 30 minutes for the stomach passage; and pH=9 for 2 hours for passage through the small intestine) resulted in an increase of the Z-averages from 77nm (PDI = 0.19) before simulated GIT passage to 112nm (PDI 0.14) after simulated stomach passage and to 275 nm (PDI 0.45) after additionally simulated passage through the small intestine (see Figure S3 SI-GAV). The results agree

with the enhanced agglomeration of TiO_2 nanoparticles when exposed to simulated gastric fluid observed by (Jones, 2015).

Biokinetics of soluble ionic ^{48}V

In the auxiliary study 99.13% and 99.31% of the applied doses of soluble ^{48}V-ions were either in the GIT or directly excreted *via* feces after 24h or 7d, respectively (see Figure S4). Only 0.87% and 0.69% of the applied ^{48}V-ion doses were absorbed across the gut epithelium. At both time points about half of the absorbed ^{48}V- ions were excreted in urine (0.44% and 0.34%, respectively). Total uptake in the organs was well below 0.1% and only the carcass consisting of skeleton and soft tissue (the latter defined as non-osseous tissues including muscles, fat, skin, connective tissue, paws) contained 0.32% and 0.24% of the ionic ^{48}V at 24h and 7d, respectively. The data on ionic ^{48}V was used to correct the biokinetics data after gavage of the [^{48}V]TiO_2NP for ^{48}V-release from the nanoparticles as described in the SI-GAV.

Biokinetics of [^{48}V]TiO_2NP

Most of the gavaged [^{48}V]TiO_2NP were directly excreted in feces (see Table 2). Only a small fraction of about 0.6% of the applied [^{48}V]TiO_2NP dose was absorbed across the intestinal barrier during the first hour after gavage. This fraction decreased to about 0.05% after 7 days as illustrated in Figure 3.

In Table 3 the raw data (%ID) are presented together with the data corrected for the radioactivity attributed to the residual blood retained in organs and tissues after exsanguination as described in the SI-GAV. Following this the activity contributions of free ^{48}V-ions were subtracted. In order to estimate this contribution we assume that all ^{48}V-activity in urinary excretion is only due to ^{48}V-ions since glomerular filtration in the kidneys prevents particles larger than 8 nm from passing into the urine (Choi, 2007). The mathematical execution of this correction is described in the SI-GAV and based on the assumption that the excretion kinetics of ionic ^{48}V is the same in the auxiliary study after application of ^{48}V-ions and in the main study with [^{48}V]TiO_2NP suspensions that may contain

or release ^{48}V-ions. The surprising result is shown in Figure S7 (supplementary Information) and shows that after 1 day the activities that can be attributed to free ^{48}V-ions and to [^{48}V]TiO_2NP are the same within the error margins.

In Table 3 the percentages of absorbed [^{48}V]TiO_2NP in all major organs, in the carcass and in the blood are presented. These data (corrected for residual blood content and ^{48}V-ions are) are visualized in Figure 4A-C. Due to the low absorption across the gut epithelium, the distribution patterns are very variable especially during the first 4h and several data at different time points were below the detection limit (DL<0.2 Bq) in spite of the high sensitivity of the radiotracer method. Nevertheless, they indicate measurable accumulation within 1 hour after gavage, which appears to be delayed in spleen, kidneys, heart and uterus where measurable accumulation could be observed only after 4h. The retention maximum was reached in spleen, kidneys and heart after 24h. Clearance mechanisms in liver, lung and blood must be effective very early and nanoparticle retention shows declining values from 4h to 7d. In all organs and tissues nanoparticle retention declined after 24h towards the end of the observation period with the exception of kidneys and brain where no further net clearance was observable. While retention in uterus and skeleton went through a maximum after 4h, showing that some net clearance can be achieved, the activity percentage retained in the brain reaches its initial value (after 1h) again after 7d indicating the least efficient clearance mechanism of all investigated organs. The kidneys also showed higher nanoparticle retention after 7d than after 4h, however passing through a maximum after 24h indicating net clearance. The largest ^{48}V-activity fraction is located in the carcass consisting of skeleton and soft tissues. Separating both compartments shows a retention in the skeleton between 0.03% and 0.15% (w/o free ^{48}V-ions) while the retention in the soft tissue declines by an order of magnitude from 0.26% after 1h to below 0.02% after 7d. Looking at the organ/tissue concentrations in %ID•g^{-1} the clearance from the skeleton is much less effective than for the soft tissue and the concentration in the skeleton is at least 10 times higher than in the soft tissue except for the 1h retention data.

The concentrations of [^{48}V]TiO_2NP per gram of organs and tissues are also provided in Table 3 and selected data are visualized in Figure 4D-F. It is remarkable how similar nanoparticle concentrations

were in each of the secondary organs over the entire time period. The nanoparticle concentration in the skeleton is of the same order of magnitude as most of the secondary organs, while in soft tissue it is considerably lower.

Distinction of the nanoparticle content in gut walls and chime

When the walls of the gut and its contents were analyzed separately, most [^{48}V]TiO_2NP were detected in the chime and only small fractions of 5.8%, 1.3%, and 0.9% in the intestinal walls, after 1h, 4h, and 24h, respectively (Figure 5). Since absorption through the gut wall to blood was <1% for all time points the data indicate either insufficient rinsing of the gut walls, or [^{48}V]TiO_2NP entrapment in mucosa, or some of the initially retained [^{48}V]TiO_2NP in the gut walls were secreted back into the gut content for excretion.

Comparison of the biokinetics of [^{48}V]TiO_2NP absorbed through the gut epithelium with the biokinetics of intravenously injected [^{48}V]TiO_2NP

In order to compare the biokinetics of [^{48}V]TiO_2NP which had been absorbed through the gut epithelium and had reached systemic circulation with those [^{48}V]TiO_2NP directly administered to the blood circulation by IV injection (Kreyling, submitted), the accumulated [^{48}V]TiO_2NP in each organ and tissue were renormalized to fractions of the nanoparticles which had been absorbed through the gut epithelium. This enables a comparison of distribution patterns of some ng of [^{48}V]TiO_2NP absorbed through the intestinal barriers with some 10000 ng [^{48}V]TiO_2NP intravenously injected. In both applications, the corresponding retention time points were studied with the same [^{48}V]TiO_2NP suspension, i.e. with the same physico-chemical properties and concentrations. Figure 6 shows the retention pattern of [^{48}V]TiO_2NP absorbed through the gut epithelium on the left side and the retention pattern of intravenously injected [^{48}V]TiO_2NP on the right side.

Discussion

This study design is associated with some shortcomings as it remains at the level of macroscopic biokinetics and does not provide any microscopic details such as any cell-type interactions with the [^{48}V]TiO_2NP in any of the secondary organs or tissues as discussed in more detail in part 1 of this study (Kreyling, submitted).

Whether food additive TiO_2 particles are *at all* absorbed in mammals following their oral ingestion is the subject of an ongoing debate (Disdier, 2015, Geraets, 2014, MacNicoll, 2015). The use of radio-labelled [^{48}V]TiO_2NP allows us, unequivocally, to address this issue. The [^{48}V]TiO_2NP proved to be sufficiently stable when exposed to aqueous acidic and peri-neutral pH environments (Hildebrand, 2015). However, due to the chemical difference between V and Ti a ^{48}V-radiolabel located on the nanoparticle surface or reaching it by diffusion in the TiO_2 matrix could be released. Alternatively, a slow dissolution process of the nanoparticles would also lead to a release of ^{48}V ions. (Hildebrand, 2015) have demonstrated that the release from proton irradiated TiO_2 (P25, Evonik) is around 2.5% after 4 h at pH = 2 and well below 1% even after 7 days at pH = 7. By reference to an auxiliary study on the ingestion of ^{48}V-ions alone, we should be able to correct for any ^{48}V-release from the [^{48}V]TiO_2NP that contributed to the analytical signal, based on the rigid, conservative assumption that all ^{48}V-activity in urine is only ionic and not particulate. Thus, while most similar in vivo studies use total Ti as a proxy for the fate of TiO_2, we have used ^{48}V as a proxy for the fate of TiO_2, which can be detected with high sensitivity. Additionally the detection of [^{48}V]TiO_2NP by γ-ray spectrometry is not affected by any chemically identical background or specimen preparation. However, the same suspensions that were applied in the intravenous study, where they showed an ionic activity contribution of at maximum 1% of the total retained activity, after gavage result in values of about 50% of free ions after 24h. They are derived from a comparison of urinary excretion data between the auxiliary and the main study and do not depend on any in-vitro assumptions on the stability of the suspensions. A reason for this difference may be a preferential absorption of ions through the epithelial GIT barrier in combination with a much more pronounced release of ^{48}V-ions from [^{48}V]TiO_2NP in the GIT environment. In agreement with Jones et al. (2015) our DLS study after simulating the ph-conditions of the GIT passage show rather aggregation than dissolution of the

nanoparticles, however a certain small-sized fraction of much smaller nanoparticles would not have been discovered by DLS and might have been absorbed and been excreted passing renal clearance. These nanoparticles would erroneously have been attributed to the ionic fraction which overestimates the corrections we apply. However, as can be seen from the data in Table 3, this would not invalidate our findings, but the retention in organs and tissues would be higher than indicated by our conservative 'corrected' data.

By evaluating the nanoparticle distribution in the whole animal and its excretions a quantitatively balanced biokinetics was obtained, whereas other groups have focused on specific organs without paying attention to the nanoparticle balance. For the first time differences between effectively administered doses and nominal doses loaded into syringes could be noted, quantified and considered. The radiotracer method revealed that up to 50% of the suspended [^{48}V]TiO_2NP dose to be administered was retained in minimal-dead-space-syringes and cannulas, presumably due to electrostatic adhesion of nanoparticles to plastic surfaces. Such effects are likely to occur in other nanoparticle suspensions as well. They are highly variable, difficult to detect and most likely depend on the materials used and their handling. They might be one reason for variations in reported results.

Our data confirm that already 1h following oral application ≈0.6% of the administered [^{48}V]TiO_2NP had passed through the gastrointestinal tract, reached systemic circulation and were retained in various organs and tissues. The fraction retained in the body (excluding the gastrointestinal tract) dropped within 4h after application to a level of ≈0.2%. This implies that not only absorption but also early excretion mechanisms for [^{48}V]TiO_2NP must be active.

To be absorbed across the gut and into the body, [^{48}V]TiO_2NP must first pass the epithelial layer. This may be via M-cell capture (Powell, 1996) or regular epithelial cell endocytosis of the small nanoparticle fraction (< 40 nm size) (Howe, 2014), or by "persorption" through holes left in villus tips as enterocytes are shed. It may even be due to 'reach out' of intestinal dendritic cells, sampling directly from the lumen. Once having passed the epithelial barrier, [^{48}V]TiO_2NP may then move

from the gut to the "body" most likely via the lymphatic network, either as particles alone or within migrating phagocytic cells (Bockmann, 2000, Pele, 2015).

Nonetheless, based upon the presented data, a fraction of absorbed particles clearly reaches the bloodstream possibly *via* the lymphatic thoracic duct into circulation. We assume that direct entry of [^{48}V]TiO_2NP into gut capillaries is less likely to occur as even large pore permeability via this route is restricted to smaller macromolecules. In contrast, nanoparticle entry into alveolar capillaries has been frequently described after lung administration (Berry, 1977) (Geiser, 2013, Geiser, 2005, Geiser, 2014). Therefore, [^{48}V]TiO_2NP surface modification by proteins and/or biomolecules seems to play a minor role for the transport of gut-absorbed nanoparticles towards circulation. In this respect it is important to note that the distribution of the [^{48}V]TiO_2NP in the various organs differs greatly between IV-injection and oral application. The difference must be related to dose and/or "pathway" of entry. Regarding dose, most local tissues and the blood itself have only a relatively low capacity for acute particle uptake via their mononuclear phagocytic system (MPS). In contrast, the liver has a high capacity. The 100-fold higher IV-injected doses saturate the local particle uptake capacity directly after administration in most organs and tissues except the liver which collects almost all of the [^{48}V]TiO_2NP. This is precisely what is seen for intravenously delivered [^{48}V]TiO_2NP. In contrast, the gut barrier acts to greatly reduce the particulate dose absorbed whilst the cellular and lymphatic systems described above serve to further limit vascular exposure to [^{48}V]TiO_2NP. Strikingly, almost all retained [^{48}V]TiO_2NP beyond the gut are in the organ free carcass and are only very gradually released over 7 days. Retention in lymph nodes may possibly explain this, however [^{48}V]TiO_2NP concentrations in samples of pure hind leg muscle with little lymphoid tissue corresponded well with the integral [^{48}V]TiO_2NP concentration of soft tissue. The very low levels of [^{48}V]TiO_2NP that do gradually reach the circulation then appear to impact all of the vascular organs to some extent presumably because their MPS is not saturated at these doses and kinetics of [^{48}V]TiO_2NP arrival. The likely influence of the protein corona remains speculative since no *in vivo* data on the protein corona of nanoparticles absorbed through the gut are available.

Another interesting feature is the slowly decreasing nanoparticle retention in most organs and tissues. The total nanoparticle retention in the body of about 0.2% after 4h decreases to about 0.05% during the 7-day period. This hints that there may be little transport from the retention sites in the parenchyma of various organs and tissues, pointing to a kind of equilibrium between the organ concentrations and the [^{48}V]TiO_2NP circulating in the blood.

The data presented here emphasize that the absorbed fraction of TiO_2NP across the intestinal epithelium of the GIT is very low (≈0.6% of the administered dose after 1h and ≈0.2% after 4h), and absorbed fractions in organs like liver and spleen are even an order of magnitude lower. The low uptake of ingested [^{48}V]TiO_2NP contrasts with the results obtained on polystyrene nanoparticles (Hussain, 1998) but agrees with our previous study using monodisperse gold nanoparticles (AuNP) of various sizes ranging from 1.4 nm to 200 nm (Schleh, 2012) and with an earlier study using polylysine-lipid dendrimers (Florence, 2000). Previous quantitative uptake studies for TiO_2 have only considered submicron and micro-particles and showed much greater absorption and peripheral distribution (Jani, 1994a). As recently discussed by Powell and co-workers, particle type and several physico-chemical nanoparticle properties may be critical determinants of nanoparticles uptake in the gut (Powell, 2010).

The observed difference between an absorbed fraction of ≈0.6% of our 70 nm anatase TiO_2NP and of 12% for gavaged 500 nm rutile TiO_2 particles found by Jani and coworkers is quite remarkable (Jani, 1994b). Whether the different particle sizes and/or the different crystalline phases, or the strikingly different doses of tens of µg per rat *versus* ≈3 mg•d^{-1} per rat applied over 10 days, or the different detection techniques employed are responsible for these large differences remains to be determined.

After 24h the absorption of [^{48}V]TiO_2NP observed in the present study was six-fold ($p<0.01$), higher than that of similar sized, monodisperse spherical AuNP (hydrodynamic diameter 85 nm) used in a previous study (Schleh, 2012).

Although it is known that absorption of nanoparticles depends largely on size (Hillery, 1994, Jani, 1994a, Schleh, 2012, Sonavane, 2008), the two nanoparticle preparations of [^{48}V]TiO_2NP and AuNP

with a similar size differ significantly in the amount of absorption. One explanation could be that the TiO_2 agglomerates break up in the digestive environment of the GIT resulting in a fraction of [^{48}V]TiO_2NP of primary particle size of 7-10 nm, which would probably absorb to a much greater extent. The effect of the digestive conditions in the stomach and small bowel environment on the stability of our TiO_2NP suspension was simulated by incubating the TiO_2NP suspension for 30min at pH-2 followed by 2 hours at pH-9. Although we neglected constituents like digestive enzymes and proteins, this simple assay was a first attempt to estimate the pH-effect of the GIT on nanoparticle stability. The measurements of the hydrodynamic diameter after incubation indicated that the average TiO_2 agglomerate size increased slightly after incubation in simulated stomach conditions (~120nm) and agglomeration continued further in simulated intestinal conditions (~250nm) (see Figure S3). Thus, in agreement with (Jones, 2015) who used simulated gastric fluid for such simulations, a breakup of TiO_2 agglomerates cannot be responsible for the higher absorption with respect to similar sized AuNP. Hence, the absorption of Au and TiO_2 nanoparticles across intestinal membranes depends not only on size but also on the nanoparticle material, and possibly other factors such as shape, state of aggregation/agglomeration, surface charge, *etc*., which have also been shown to influence the biodistribution of nanoparticles (Arnida, 2010, Devarajan, 2010).

Regarding the biokinetics and accumulation of nanoparticles in secondary organs and tissues, the peak of retained [^{48}V]TiO_2NP was found after 1 hour, with a maximum retention of 0.53% in the carcass, i.e., in adipose tissue, skeleton, skin, and muscles. This finding is not surprising considering that nanoparticles are able to penetrate adipocytes (Vaijayanthimala, 2009) or muscle cells (Suh, 1998, Zhang, 2009) that account for most of the carcass mass. Only small and heterogeneous amounts were found in the lungs and other organs.

Earlier we performed another set of studies comparing IV-injection and gavage using a set of six different-sized, monodisperse, virtually insoluble AuNP (1.4 nm, 2.8 nm, 5 nm, 18 nm, 80 nm, and 200 nm) (Hirn, 2011, Schleh, 2012). The present results are in qualitative agreement with these studies. For instance, also AuNP were predominantly retained in the liver after IV-injection while liver retention was ten-fold lower after absorption through the gut. Additionally, after gavage the

retained AuNP in the carcass dominated the biodistribution pattern, similar to the pattern for [^{48}V]TiO_2NP shown in Figure 6.

Importantly, low but unambiguously detectable amounts of [^{48}V]TiO_2NP were found in the brain and in the uterus where they were still detectable after 7 days. Although brain and uterus have tight barriers, [^{48}V]TiO_2NP entry appears to be possible although we cannot exclude nanoparticle entrapment in vascular endothelia. Similar but even lower retention in the brain was found for 80 nm AuNP (Schleh, 2012). Whether the nanoparticle uptake results from intracellular nanoparticle transport in the circulation and/or uptake of extracellularly circulating nanoparticles (surface-modified by blood proteins and/or biomolecules) cannot be decided from both of our studies. Only the studies of Disdier et al. (Disdier, 2015) on the interaction of nanoparticles with the brain by using an *in vitro* blood-brain-barrier model in addition to their animal experiments have claimed to show blood-brain-barrier crossing of TiO_2 nanoparticles in rats after oral intake. We also note that we have previously found a 10- to 100-fold enhanced accumulation of 15 nm sized AuNP in lungs, spleen, kidneys, heart and brain, and to a lesser extent in the liver, between 0.5h and 48h after IV-injection of AuNP that were firmly conjugated with albumin as compared to non-conjugated, citrate-stabilized AuNP of the same core size and applied dose (Schäffler, 2014). These results indicate that the MPS in the various organs and blood appears to respond to biomolecular AuNP surface-modifications and cause strong changes in the accumulation pattern as early as 0.5h after application. Slightly lower enhancements (2 to 20-fold) were found when the AuNP were pre-conjugated with apolipoprotein-E. We recognize that the quantity of nanoparticles found in many organs and especially the brain is very low. However, considering that, in many countries, several milligrams of TiO_2 are ingested per person per day over decades and given the high biopersistence of TiO_2, long term accumulation cannot be excluded. Indeed, while there is some evidence for a moderate or low short-term risk at high enough TiO_2 oral doses, long-term biokinetics and toxicological NP studies are still lacking but would be most important for a rational long-term low dose risk assessment.

Conclusions

We have shown that the absorption of nanosized TiO_2NP across the intestinal membrane is low (less than 0.6% of the applied dose) but not negligible. Absorption in the gut seems to depend not only on size but also on the nanoparticle material, and probably other physico-chemical factors.

Seven days after oral application most organs still retain a fraction larger than 0.001% of the applied dose which corresponds to about 10^7-10^8 nanoparticles. In view of the apparently slow excretion kinetics a gradual, and possibly undesirable, accumulation of absorbed, systemically circulating particles in certain cells and organs seems to be a strong possibility for subjects chronically exposed to TiO_2 nanoparticles.

Comparing the biodistribution of [^{48}V]TiO_2-nanoparticles retained after passage through the gastro-intestinal barrier with the biodistribution determined after intravenous injection in Part 1 of this study, the biokinetics patters are very different. Thus, intravenous injection appears not to be an adequate surrogate for assessing the biodistribution and potential health effects occurring after oral exposure to TiO_2 nanoparticles. The differences probably depend on the doses that reach systemic circulation, the dose rates and possibly the "pathway" of entry into circulation. The effect of the protein corona of the nanoparticles obtained after different routes of application and the effect on the biological response need to be clarified by further dedicated investigations.

ACKNOWLEDGMENTS

We are most grateful for in-depth discussions with Prof. Dr. J. Powell and Dr. L. Pele from Cambridge University, MRC Human Nutrition Research, about the physiology of nanoparticle transport from the gut towards blood circulation. We also thank Sebastian Kaidel, Paula Mayer and Nadine Senger from Helmholtz Center Munich for their excellent technical assistance, as well as Antonio Bulgheroni, Kamel Abbas, Federica Simonelli, Izabela Cydzik, and Giulio Cotogno from the EU-Joint Research Center who strongly supported the nanoparticle radio-labeling task. We also express our sincere gratitude to Barbara Rothen-Rutishauser and David Raemy, University of Fribourg, Switzerland, who performed the TEM analysis of the TiO_2NP.

Declaration of Interest

The authors declare that they have no financial, consulting, and personal relationships with other people or organizations that could influence (bias) the author's work.

This work was partially supported by the German Research Foundation SPP 1313, the EU-FP6 project Particle-Risk (012912 (NEST)), and the EU FP7 projects NeuroNano (NMP4-SL- 2008-214547), ENPRA (NMP4-SL-2009-228789) and InLIveTox (NMP-2008-1.3-2 CP-FP 228625-2).

Supplementary Material available online.

- Radio-labeling of titanium dioxide (TiO_2) nanoparticles
- Nanoparticle preparation for application and nanoparticle characterization
- Influence of the acidic and basic environment of the GIT on possible de-agglomeration of TiO_2NP
- Animals
- Nanoparticle application and animal maintenance in metabolic cages
- Sample preparation for radiometric analysis
- Radiometric and statistical analysis
- Distinction between gut walls and content
- Blood correction
- ^{48}V activity determination of skeleton and soft tissue
- Biokinetics of soluble ^{48}V in ionic form after intra-esophagal instillation / gavage
- Correction of the biokinetics assigned to [^{48}V]TiO_2NP for the effect of free ^{48}V ions

References

Arnida, A, Janat-Amsbury, MM, Ray, A, Peterson, CM & Ghandehari, H 2010. Geometry and surface characteristics of gold nanoparticles influence their biodistribution and uptake by macrophages. *Eur J Pharm Biopharm*.

Berry, JP, Arnoux, B, Stanislas, G, Galle, P & Chretien, J 1977. A microanalytic study of particles transport across the alveoli: role of blood platelets. *Biomedicine,* 27**,** 354-7.

Bockmann, J, Lahl, H, Eckert, T & Unterhalt, B 2000. [Blood titanium levels before and after oral administration titanium dioxide]. *Pharmazie,* 55**,** 140-3.

Choi, HS, Liu, W, Misra, P, Tanaka, E, Zimmer, JP, Ipe, BI, Bawendi, MG & Frangioni, JV 2007. Renal clearance of quantum dots. *Nature Biotechnology,* 25**,** 1165-1170.

Devarajan, PV, Jindal, AB, Patil, RR, Mulla, F, Gaikwad, RV & Samad, A 2010. Particle shape: a new design parameter for passive targeting in splenotropic drug delivery. *J Pharm Sci,* 99**,** 2576-81.

Disdier, C, Devoy, J, Cosnefroy, A, Chalansonnet, M, Herlin-Boime, N, Brun, E, Lund, A & Mabondzo, A 2015. Tissue biodistribution of intravenously administrated titanium dioxide nanoparticles revealed blood-brain barrier clearance and brain inflammation in rat. *Part Fibre Toxicol,* 12**,** 27.

Florence, AT, Sakthivel, T & Toth, I 2000. Oral uptake and translocation of a polylysine dendrimer with a lipid surface. *Journal of Controlled Release,* 65**,** 253-9.

Geiser, M, Quaile, O, Wenk, A, Wigge, C, Eigeldinger-Berthou, S, Hirn, S, Schaffler, M, Schleh, C, Moller, W, Mall, MA & Kreyling, WG 2013. Cellular uptake and localization of inhaled gold nanoparticles in lungs of mice with chronic obstructive pulmonary disease. *Part Fibre Toxicol,* 10**,** 19.

Geiser, M, Rothen-Rutishauser, B, Kapp, N, Schurch, S, Kreyling, W, Schulz, H, Semmler, M, Im Hof, V, Heyder, J & Gehr, P 2005. Ultrafine particles cross cellular membranes by nonphagocytic mechanisms in lungs and in cultured cells. *Environmental Health Perspectives,* 113**,** 1555-60.

Geiser, M, Stoeger, T, Casaulta, M, Chen, S, Semmler-Behnke, M, Bolle, I, Takenaka, S, Kreyling, WG & Schulz, H 2014. Biokinetics of nanoparticles and susceptibility to particulate exposure in a murine model of cystic fibrosis. *Part Fibre Toxicol,* 11**,** 19.

Geraets, L, Oomen, AG, Krystek, P, Jacobsen, NR, Wallin, H, Laurentie, M, Verharen, HW, Brandon, EF & De Jong, WH 2014. Tissue distribution and elimination after oral and intravenous administration of different titanium dioxide nanoparticles in rats. *Part Fibre Toxicol,* 11**,** 30.

Hildebrand, H, Schymura, S, Holzwarth, U, Gibson, N, Dalmiglio, M & Franke, K 2015. Strategies for radiolabeling of commercial TiO2 nanopowder as a tool for sensitive nanoparticle detection in complex matrices. *Journal of Nanoparticle Research,* 17**,** 1-12.

Hillery, AM, Jani, PU & Florence, AT 1994. Comparative, quantitative study of lymphoid and non-lymphoid uptake of 60 nm polystyrene particles. *J Drug Target,* 2**,** 151-6.

Hirn, S, Semmler-Behnke, M, Schleh, C, Wenk, A, Lipka, J, Schaffler, M, Takenaka, S, Moller, W, Schmid, G, Simon, U & Kreyling, WG 2011. Particle size-dependent and surface charge-dependent biodistribution of gold nanoparticles after intravenous administration. *European Journal of Pharmaceutics and Biopharmaceutics,* 77**,** 407-16.

Howe, SE, Lickteig, DJ, Plunkett, KN, Ryerse, JS & Konjufca, V 2014. The uptake of soluble and particulate antigens by epithelial cells in the mouse small intestine. *PLoS One,* 9**,** e86656.

Hussain, N & Florence, AT 1998. Utilizing bacterial mechanisms of epithelial cell entry: invasin-induced oral uptake of latex nanoparticles. *Pharm Res,* 15**,** 153-6.

Jani, PU, McCarthy, DE & Florence, AT 1994a. Titanium dioxide (rutile) particle uptake from the rat GI tract and translocation to systemic organs after oral administration *Int J Pharm,* 105**,** 157-168.

Jani, PU, McCarthy, DE & Florence, AT 1994b. Titanium dioxide (rutile) particle uptake from thé rat GI tract and translocation to systemic organs after oral administration. *International Journal of Pharmaceutics,* 105**,** 157-168.

Jones, K, Morton, J, Smith, I, Jurkschat, K, Harding, AH & Evans, G 2015. Human in vivo and in vitro studies on gastrointestinal absorption of titanium dioxide nanoparticles. *Toxicol Lett,* 233**,** 95-101.

Kreyling, WG, Biswas, P, Messing, ME, Gibson, N, Geiser, M, Wenk, A, Sahu, M, Deppert, K, Cydzik, I, Wigge, C, Schmid, O & Semmler-Behnke, M 2011. Generation and characterization of stable, highly concentrated titanium dioxide nanoparticle aerosols for rodent inhalation studies. *Journal of Nanoparticle Research,* 13**,** 511–524.

Kreyling, WG, Hirn, S, Moller, W, Schleh, C, Wenk, A, Celik, G, Lipka, J, Schaffler, M, Haberl, N, Johnston, BD, Sperling, R, Schmid, G, Simon, U, Parak, WJ & Semmler-Behnke, M 2014. Air-blood barrier translocation of tracheally instilled gold nanoparticles inversely depends on particle size. *ACS Nano,* 8**,** 222-33.

Kreyling, WG, Holzwarth, U, Haberl, N, Kozempel, J, Wenk, A, Hirn, S, Schleh, C, Schäffler, M, Lipka, J, Semmler-Behnke, M & Gibson, N submitted. Part 1: Quantitative biokinetics of titanium dioxide nanoparticles after intravenous injection in rats *Nanotoxicology***,** (submitted).

Lomer, MC, Hutchinson, C, Volkert, S, Greenfield, SM, Catterall, A, Thompson, RP & Powell, JJ 2004. Dietary sources of inorganic microparticles and their intake in healthy subjects and patients with Crohn's disease. *Br J Nutr,* 92**,** 947-55.

MacNicoll, A, Kelly, M, Aksoy, H, Kramer, E, Bouwmeester, H & Chaudhry, Q 2015. A study of the uptake and biodistribution of nano-titanium dioxide using in vitro and in vivo models of oral intake. *Journal of Nanoparticle Research,* 17**,** 1-20.

Oeff, K & Konig, A 1955. [Blood volume of rat organs and residual amount of blood after blood letting or irrigation; determination with radiophosphorus-labeled erythrocytes.]. *Naunyn Schmiedebergs Arch Exp Pathol Pharmakol,* 226**,** 98-102.

Pele, LC, Thoree, V, Bruggraber, SF, Koller, D, Thompson, RP, Lomer, MC & Powell, JJ 2015. Pharmaceutical/food grade titanium dioxide particles are absorbed into the bloodstream of human volunteers. *Part Fibre Toxicol,* 12**,** 26.

Peters, RJ, Van Bemmel, G, Herrera-Rivera, Z, Helsper, JP, Marvin, HJ, Weigel, S, Tromp, P, Oomen, AG, Rietveld, A & Bouwmeester, H 2014. Characterisation of titanium dioxide nanoparticles in food products: Analytical methods to define nanoparticles. *J Agric Food Chem*.

Powell, JJ, Ainley, CC, Harvey, RS, Mason, IM, Kendall, MD, Sankey, EA, Dhillon, AP & Thompson, RP 1996. Characterisation of inorganic microparticles in pigment cells of human gut associated lymphoid tissue. *Gut,* 38**,** 390-5.

Powell, JJ, Faria, N, Thomas-Mckay, E & Pele, LC 2010. Origin and fate of dietary nanoparticles and microparticles in the gastrointestinal tract. *J Autoimmun,* 34**,** J226-33.

Schäffler, M, Sousa, F, Wenk, A, Sitia, L, Hirn, S, Schleh, C, Haberl, N, Violatto, M, Canovi, M, Andreozzi, P, Salmona, M, Bigini, P, Kreyling, WG & Krol, S 2014. Blood protein coating of gold nanoparticles as potential tool for organ targeting. *Biomaterials,* 35**,** 3455-66.

Schleh, C, Semmler-Behnke, M, Lipka, J, Wenk, A, Hirn, S, Schaffler, M, Schmid, G, Simon, U & Kreyling, WG 2012. Size and surface charge of gold nanoparticles determine absorption across intestinal barriers and accumulation in secondary target organs after oral administration. *Nanotoxicology,* 6**,** 36-46.

Shi, H, Magaye, R, Castranova, V & Zhao, J 2013. Titanium dioxide nanoparticles: a review of current toxicological data. *Part Fibre Toxicol,* 10**,** 15.

Sonavane, G, Tomoda, K & Makino, K 2008. Biodistribution of colloidal gold nanoparticles after intravenous administration: effect of particle size. *Colloids Surf B Biointerfaces,* 66**,** 274-80.

Suh, H, Jeong, B, Liu, F & Kim, SW 1998. Cellular uptake study of biodegradable nanoparticles in vascular smooth muscle cells. *Pharm Res,* 15**,** 1495-8.

Tassinari, R, Cubadda, F, Moracci, G, Aureli, F, D'amato, M, Valeri, M, De Berardis, B, Raggi, A, Mantovani, A, Passeri, D, Rossi, M & Maranghi, F 2014. Oral, short-term exposure to titanium dioxide nanoparticles in Sprague-Dawley rat: focus on reproductive and endocrine systems and spleen. *Nanotoxicology,* 8**,** 654-62.

Vaijayanthimala, V, Tzeng, YK, Chang, HC & Li, CL 2009. The biocompatibility of fluorescent nanodiamonds and their mechanism of cellular uptake. *Nanotechnology,* 20**,** 425103.

Weir, A, Westerhoff, P, Fabricius, L, Hristovski, K & Von Goetz, N 2012. Titanium dioxide nanoparticles in food and personal care products. *Environ Sci Technol,* 46**,** 2242-50.

Zhang, S, Chen, X, Gu, C, Zhang, Y, Xu, J, Bian, Z, Yang, D & Gu, N 2009. The Effect of Iron Oxide Magnetic Nanoparticles on Smooth Muscle Cells. *Nanoscale Res Lett,* 4**,** 70-77.

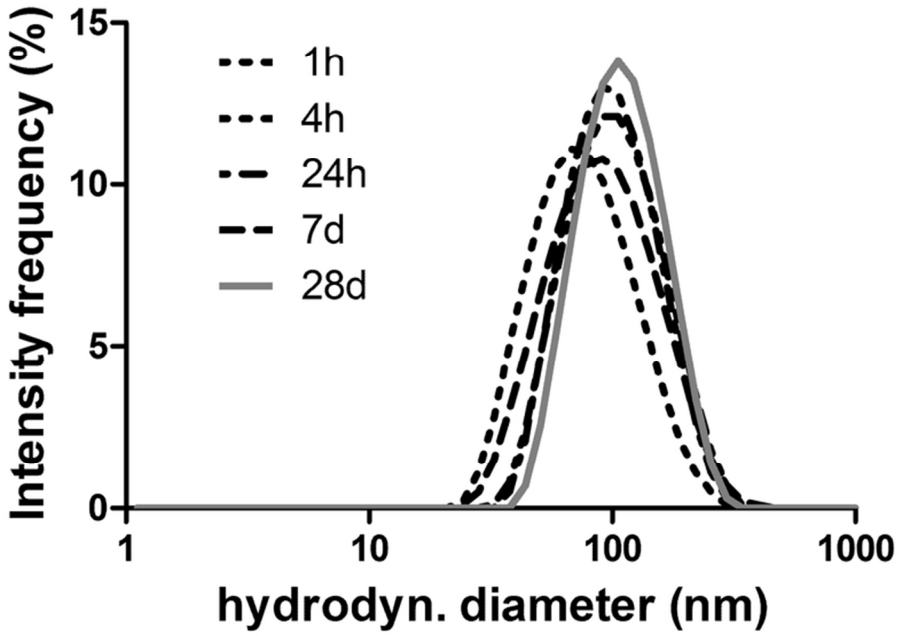

Figure 1: Hydrodynamic diameter of the four separately prepared [48V]TiO2NP suspensions used to study the four retention times of 1h, 4h, 24h and 7d (28d not studied for gavage) measured directly before esophageal instillation.

73x52mm (300 x 300 DPI)

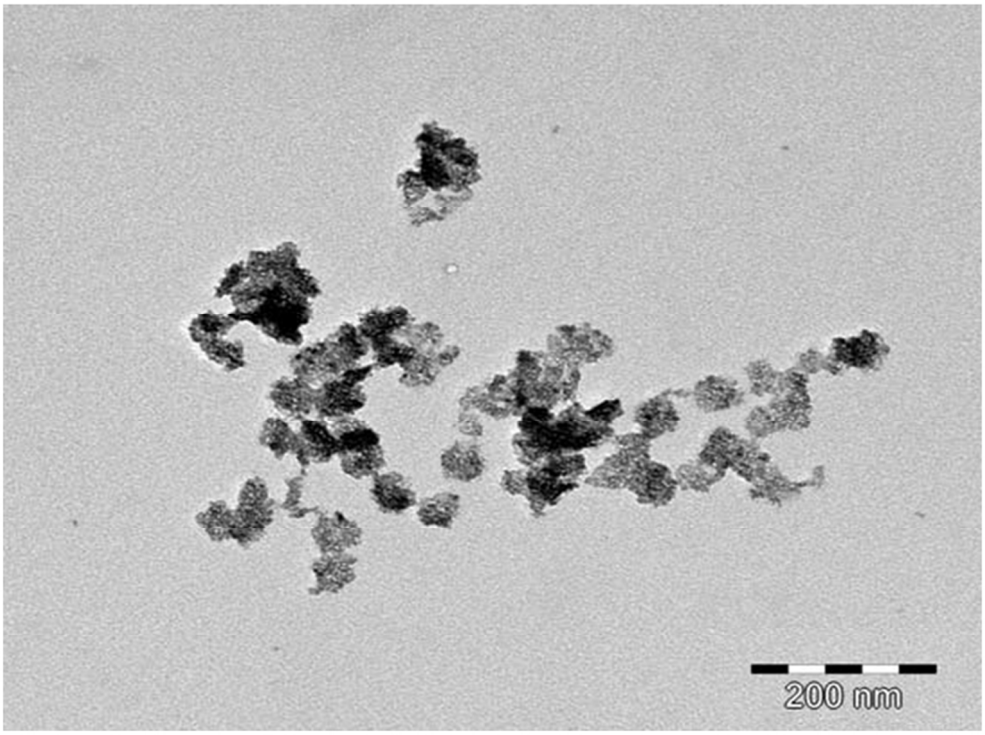

Figure 2: Transmission electron micrograph of size-selected TiO2NP sampled immediately after the size-selection procedure. TEM sample preparation leads to 'clumping' together of aggregates/agglomerates on the support grid.

254x190mm (96 x 96 DPI)

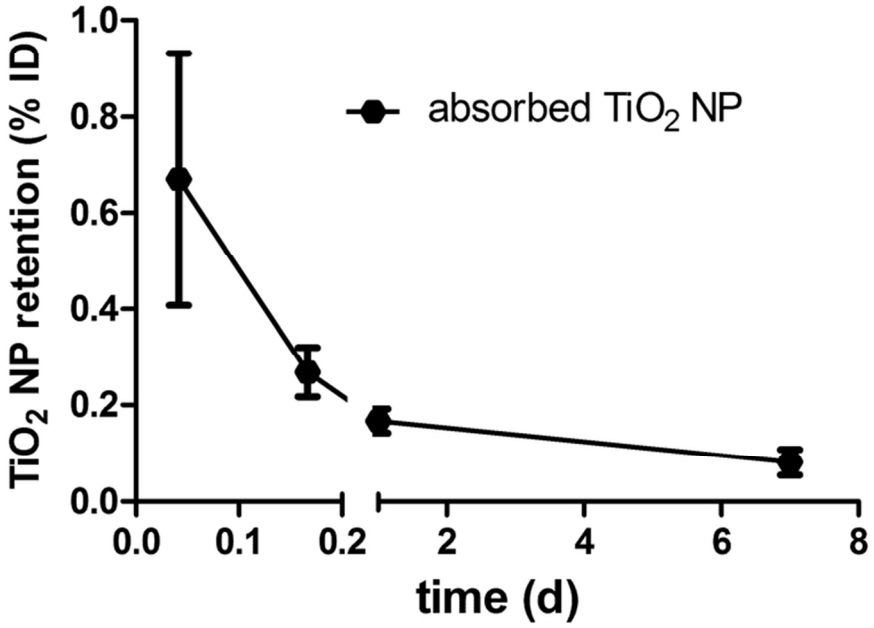

Figure 3: Fractions of the applied 48V-activity that were absorbed through the gut walls, entered systemic circulation and accumulated in secondary organs and tissues. Mean ± SEM of n=4 rats at each time point.

73x52mm (300 x 300 DPI)

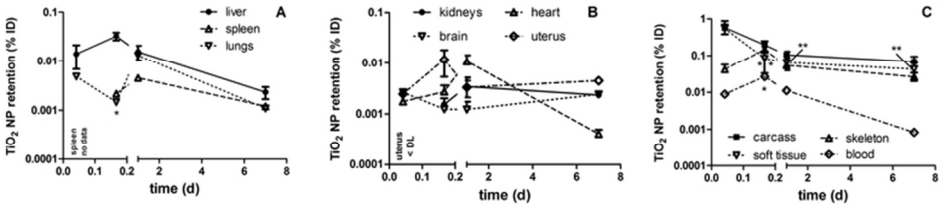

Figure 4-1: Quantified 48V-activity levels, reported as percent of applied [48V]TiO2NP dose (% ID) in various organs and tissues and in total blood at 1h, 4h, 24h and 7d after gavage in panels A-C and concentrations (%ID•g-1 of organ or tissue) in panels D-F. The [48V]TiO2NP content in the residual blood of each organ or tissue was subtracted and additionally the activity attributed to 48V-ion released from the nanoparticles. Mean ± SEM of n=4 rats at each time point. Significant difference from [48V]TiO2NP retention at 1h: $p<0.05$ (*);$p<0.01$ (**).

70x17mm (300 x 300 DPI)

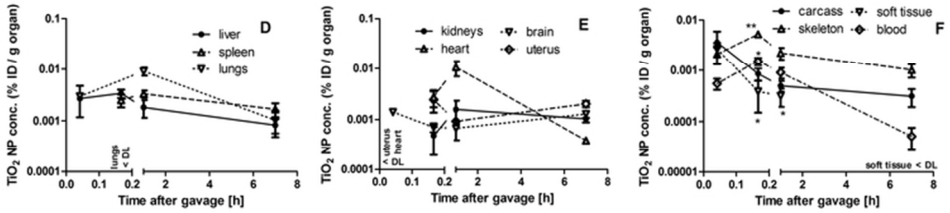

Figure 4-2: Quantified 48V-activity levels, reported as percent of applied [48V]TiO2NP dose (% ID) in various organs and tissues and in total blood at 1h, 4h, 24h and 7d after gavage in panels A-C and concentrations (%ID•g-1 of organ or tissue) in panels D-F. The [48V]TiO2NP content in the residual blood of each organ or tissue was subtracted and additionally the activity attributed to 48V-ion released from the nanoparticles. Mean ± SEM of n=4 rats at each time point. Significant difference from [48V]TiO2NP retention at 1h: p<0.05 (*);p<0.01 (**).‼ ┼ ‼ ┼ (##One legend for both Figures 4-1 GAV and 4-2 GAV)

67x17mm (300 x 300 DPI)

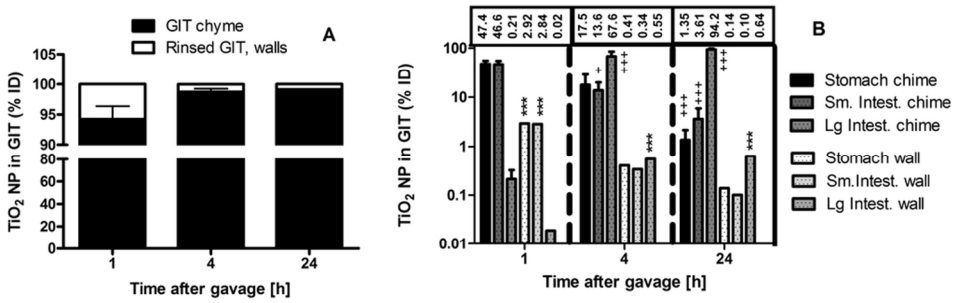

Figure 5: Fractions of [48V]TiO2NP detected in the gastrointestinal tract. (A) Differentiation of [48V]TiO2NP in the total chime and the GIT walls (5.8%, 1.3%, and 0.9%); (B) fractions of [48V]TiO2NP in the chime and walls of each of the three compartments of the GIT. Mean ± SEM of n=4 rats at each time point. Significant difference from [48V]TiO2NP retention between chime versus wall of compartment: $p<0.05$ (*);$p<0.01$ (**); $p<0.001$ (***); significant difference from [48V]TiO2NP retention at 1h for chime or wall of each compartment: $p<0.05$ (+);$p<0.01$ (++);$p<0.001$ (+++) .

91x31mm (300 x 300 DPI)

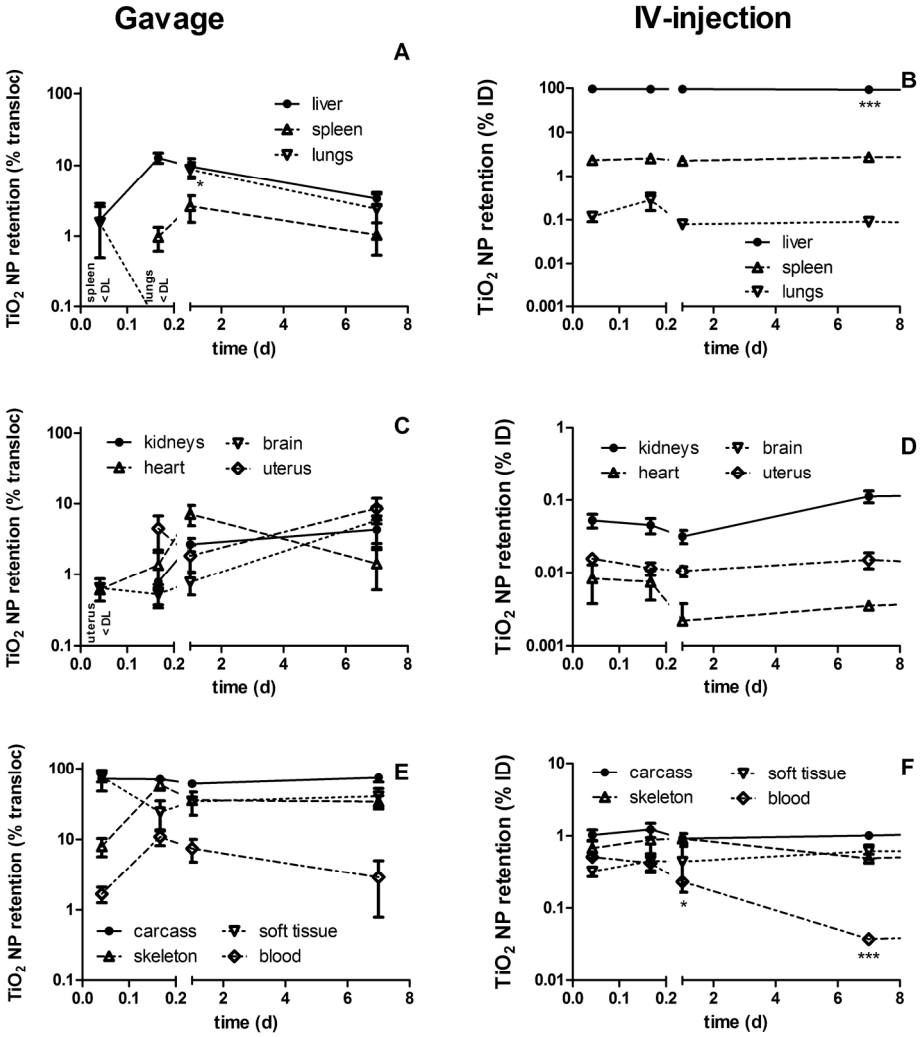

Figure 6: Comparison of [48V]TiO2NP retention and accumulation in secondary organs and tissues after gavage and intravenous injection (Part 1; (Kreyling, submitted). Panel A and B: liver, spleen, lungs; panels C and D: kidneys, heart, uterus, brain; panels E and F: carcass, skeleton, soft tissue and blood. Note that any missing data indicate fractions below the detection limit. Mean ± SEM of n=4 rats at each time point.

198x215mm (300 x 300 DPI)

Table 1: Physico-chemical properties of the [^{48}V]TiO_2NP suspensions used for the four different retention times studied by gavage and the mean values of the applied ^{48}V activity (kBq) and mass (µg) of [^{48}V]TiO_2NP effectively received by the rats. Also the mean doses in µg/g BW are given. Additionally, [^{48}V]TiO_2NP losses in the syringe and/or cannula are provided as detailed in SI-GAV.

Retention time		1h	4h	24h	7d
Zeta Potential	[mV]	-38.9 ± 4.2	-33.2 ± 2.4	-29.9 ± 8.1	-42.7 ± 9.2
Z-average	[nm]	93	72	93	82
PDI		0.157	0.228	0.160	0.197
Effective ^{48}V radioactivity received by rats	[kBq]	13.07 ± 1.22	8.53 ± 0.34	12.22 ± 1.34	67.24 ± 6.38
applied [^{48}V]TiO_2NP mass	[µg]	13.07 ± 1.22	8.53 ± 0.34	12.22 ± 1.34	28.61 ± 2.71
Mean applied dose	[µg•kg^{-1} BW]	49.82 ± 4.6	30.8 ± 0.99	44.44 ± 2.41	78.0 ± 10.4
Percentage of [^{48}V]TiO_2NP retained in the syringe after administration^{+}	[%]	51 ± 14	38 ± 6	12 ± 4	n.d.

Table 2: Percentages of [^{48}V]TiO_2NP, detected in the GIT and feces

	[^{48}V]TiO_2NP percentages (% ID) in GIT and feces		
Time After Application	Administered ^{48}V radio-activity [kBq]	GIT + Internal feces	Excreted feces
1 h	13.07 ± 1.22	99.3 ± 0.02	No excretion
4 h	8.53 ± 0.34	99.7 ± 0.02	No excretion
24 h	12.22 ± 1.34	22.1 ± 3.1	77.4 ± 3.1
7 d	67.24 ± 6.38	0.00 ± 0.00	99.7 ± 0.01

Table 3: [^{48}V]TiO_2NP retention in organs and tissues 1h, 4h, 24h and 7d after gavage. The raw data are presented as retained percentage of the applied activity of [^{48}V]TiO_2NP (% ID, corrected for decay). The data values after correction for the [^{48}V]TiO_2NP content in the residual blood present in organs and tissues after exsanguination (without (w/o) residual blood content) and additionally for the contributions of free ^{48}V-ions to the biodistribution (w/o free ^{48}V) are also shown. After these corrections the ^{48}V-activity data were converted into [^{48}V]TiO_2NP concentrations per mass of organ or tissue, given as % ID/g and in ng•g^{-1}. Since the applied [^{48}V]TiO_2NP doses varied and also were intentionally increased for the 7d group most mass concentrations in ng•g^{-1} exhibit an increase from 24h to 7d. The values in % ID/g are independent of the applied doses. (< DL = below detection limit). In the last line "% absorbed TiO_2" the [^{48}V]TiO_2NP fractions were normalized to those [^{48}V]TiO_2NP which had entered blood circulation; see Supp-GAV.

organ	retention time (d)	1h mean ± SEM	4h mean ± SEM	24h mean ± SEM	7d mean ± SEM
liver	raw data (% ID)	0.016 ± 0.005	0.036 ± 0.006	0.023 ± 0.005	0.007 ± 0.002
liver	w/o resid. blood cont.	0.015 ± 0.005	0.032 ± 0.005	0.019 ± 0.004	0.006 ± 0.002
liver	w/o free ^{48}V	0.013 ± 0.005	0.031 ± 0.005	0.013 ± 0.004	0.002 ± 0.0006
liver	TiO_2 conc. (% ID/g tiss.)	0.0025 ± 0.0001	0.0032 ± 0.0005	0.0015 ± 0.0006	0.0008 ± 0.0003
liver	TiO_2 conc. (ng/g tiss.)	0.21 ± 0.08	0.27 ± 0.04	0.17 ± 0.06	0.092 ± 0.034
liver	% absorbed TiO_2	2.16 ± 2.16	12.5 ± 4.1	9.5 ± 5.4	3.25 ± 1.40
spleen	raw data (% ID)	< DL	0.0024 ± 0.0005	0.0041 ± 0.0014	0.0016 ± 0.0006
spleen	w/o resid. blood cont.	< DL	0.0021 ± 0.0006	0.0036 ± 0.0013	0.0015 ± 0.0005
spleen	w/o free ^{48}V	< DL	0.0021 ± 0.0006	0.0032 ± 0.0012	0.0012 ± 0.0003
spleen	TiO_2 conc. (% ID/g tiss.)	< DL	0.0024 ± 0.0006	0.0025 ± 0.0002	0.0017 ± 0.0004
spleen	TiO_2 conc. (ng/g tiss.)	< DL	0.21 ± 0.06	0.35 ± 0.08	0.45 ± 0.13
spleen	% absorbed TiO_2	< DL	0.95 ± 0.60	2.58 ± 2.12	0.99 ± 0.67
kidneys	raw data (% ID)	< DL	0.0028 ± 0.0005	0.0078 ± 0.002	0.0069 ± 0.002
kidneys	w/o resid. blood cont.	< DL	0.0015 ± 0.0006	0.0065 ± 0.0015	0.0064 ± 0.0017
kidneys	w/o free ^{48}V	< DL	0.0011 ± 0.0006	0.0038 ± 0.0013	0.0023 ± 0.0004
kidneys	TiO_2 conc. (% ID/g tiss.)	< DL	0.0004 ± 0.0002	0.0017 ± 0.0006	0.001 ± 0.0001
kidneys	TiO_2 conc. (ng/g tiss.)	< DL	0.037 ± 0.020	0.198 ± 0.055	0.289 ± 0.048
kidneys	% absorbed TiO_2	< DL	0.77 ± 0.67	2.61 ± 0.96	4.11 ± 3.02
lungs	raw data (% ID)	0.038 ± 0.031	0.0003 ± 0.0001	0.012 ± 0.002	0.0012 ± 0.0005
lungs	w/o resid. blood cont.	0.032 ± 0.025	< DL	0.011 ± 0.002	0.0012 ± 0.0005
lungs	w/o free ^{48}V	0.031 ± 0.025	< DL	0.011 ± 0.002	0.0011 ± 0.0001
lungs	TiO_2 conc. (% ID/g tiss.)	0.021 ± 0.017	< DL	0.007 ± 0.002	0.001 ± 0.0004
lungs	TiO_2 conc. (ng/g tiss.)	2.38 ± 1.94	< DL	0.72 ± 0.32	0.10 ± 0.03
lungs	% absorbed TiO_2	1.97 ± 2.31	< DL	8.57 ± 4.42	2.30 ± 2.49
heart	raw data (% ID)	< DL	0.0031 ± 0.001	0.0085 ± 0.0024	0.0003 ± 0.0002
heart	w/o resid. blood cont.	< DL	0.0026 ± 0.0009	0.0081 ± 0.0024	0.0003 ± 0.0002
heart	w/o free ^{48}V	< DL	0.0026 ± 0.0009	0.008 ± 0.0024	< DL
heart	TiO_2 conc. (% ID/g tiss.)	< DL	0.0026 ± 0.001	0.0079 ± 0.0024	< DL
heart	TiO_2 conc. (ng/g tiss.)	< DL	0.247 ± 0.096	0.647 ± 0.341	< DL
heart	% absorbed TiO_2	< DL	1.32 ± 1.39	6.97 ± 4.43	< DL
brain	raw data (% ID)	0.0025 ± 0.0002	0.0014 ± 0.0001	0.00123 ± 0.0005	0.0028 ± 0.0003
brain	w/o resid. blood cont.	0.0024 ± 0.0001	0.0012 ± 0.0001	0.001 ± 0.0004	0.0027 ± 0.0003
brain	w/o free ^{48}V	0.0024 ± 0.0001	0.0012 ± 0.0001	0.001 ± 0.0004	0.0024 ± 0.0004
brain	TiO_2 conc. (% ID/g tiss.)	0.0012 ± 0.0001	0.0007 ± 0.0001	0.0006 ± 0.0002	0.0013 ± 0.0002

brain	TiO_2 conc. (ng/g tiss.)	0.163 ± 0.010	0.057 ± 0.008	0.063 ± 0.021	0.360 ± 0.074
brain	% absorbed TiO_2	0.82 ± 0.56	0.51 ± 0.26	0.76 ± 0.44	5.52 ± 6.43
uterus	raw data (% ID)	< DL	0.012 ± 0.005	0.0027 ± 0.0009	0.0046 ± 0.0004
uterus	w/o resid. blood cont.	< DL	0.011 ± 0.004	0.0024 ± 0.0008	0.0044 ± 0.0002
uterus	w/o free ^{48}V	< DL	0.011 ± 0.004	0.0024 ± 0.0008	0.0044 ± 0.0002
uterus	TiO_2 conc. (% ID/g tiss.)	< DL	0.002 ± 0.001	0.0007 ± 0.0001	0.002 ± 0.0003
uterus	TiO_2 conc. (ng/g tiss.)	< DL	0.197 ± 0.057	0.082 ± 0.011	0.554 ± 0.048
uterus	% absorbed TiO_2	< DL	4.36 ± 3.10	1.80 ± 1.30	8.16 ± 6.44
blood	raw data (% ID)	0.008 ± 0.002	0.0252 ± 0.0042	0.0202 ± 0.0054	0.0015 ± 0.0001
blood	w/o resid. blood cont.	0.008 ± 0.002	0.0252 ± 0.0042	0.0202 ± 0.0054	0.0015 ± 0.0001
blood	w/o free ^{48}V	0.0045 ± 0.0015	0.0112 ± 0.009	0.0081 ± 0.0028	0.0008 ± 0.0003
blood	TiO_2 conc. (% ID/g tiss.)	0.0003 ± 0.0001	0.0015 ± 0.0003	0.0009 ± 0.0002	0.0001 ± 0
blood	TiO_2 conc. (ng/g tiss.)	0.037 ± 0.013	0.161 ± 0.053	0.064 ± 0.023	0.015 ±0.006
blood	% absorbed TiO_2	2.14 ± 1.05	10.68 ± 5.37	7.24 ± 5.16	2.75 ± 3.47
carcass	raw data (% ID)	0.567 ± 0.275	0.207 ± 0.052	0.154 ± 0.029	0.076 ± 0.028
carcass	w/o resid. blood cont.	0.565 ± 0.275	0.199 ± 0.052	0.149 ± 0.028	0.075 ± 0.028
carcass	w/o free ^{48}V	0.530 ± 0.281	0.188 ± 0.053	0.081 ± 0.019	0.029 ± 0.011
carcass	TiO_2 conc. (% ID/g tiss.)	0.003 ± 0.002	0.0008 ± 0.0002	0.0004 ± 0.0001	0.0001 ± 0.0001
carcass	TiO_2 conc. (ng/g tiss.)	0.327 ± 0.178	0.067 ± 0.019	0.045 ± 0.009	0.036 ± 0.012
carcass	% absorbed TiO_2	91.3 ± 59.9	69.0 ± 12.0	59.3 ± 11.6	71.0 ± 19.7
skeleton	raw data (% ID)	0.048 ± 0.012	0.143 ± 0.006	0.055 ± 0.011	0.03 ± 0.009
skeleton	w/o resid. blood cont.	0.048 ± 0.012	0.142 ± 0.006	0.054 ± 0.011	0.03 ± 0.009
skeleton	w/o free ^{48}V	0.038 ± 0.013	0.139 ± 0.007	0.044 ± 0.008	0.026 ± 0.008
skeleton	TiO_2 conc. (% ID/g tiss.)	0.0019 ± 0.0007	0.005 ± 0.0003	0.0054 ± 0.0036	0.001 ± 0.0003
skeleton	TiO_2 conc. (ng/g tiss.)	0.25 ± 0.10	0.43 ± 0.03	0.21 ± 0.04	0.29 ± 0.09
skeleton	% absorbed TiO_2	8.7 ± 5.0	49.0 ± 17.0	30.4 ± 6.9	32.4 ± 13.8
soft tissue	raw data (% ID)	0.519 ± 0.267	0.065 ± 0.035	0.094 ± 0.025	0.04 ± 0.094
soft tissue	w/o resid. blood cont.	0.516 ± 0.266	0.063 ± 0.032	0.086 ± 0.024	0.039 ± 0.087
soft tissue	w/o free ^{48}V	0.263 ± 0.124	0.029 ± 0.024	0.046 ± 0.016	0.019 ± 0.034
soft tissue	TiO_2 conc. (% ID/g tiss.)	0.003 ± 0.001	0.0003 ± 0.0002	0.0005 ± 0.0002	0.0002 ± 0.0001
soft tissue	TiO_2 conc. (ng/g tiss.)	0.38 ± 0.15	0.028 ± 0.015	0.024 ± 0.007	0.06 ± 0.027
soft tissue	% absorbed TiO_2	82.8 ± 21.0	19.9 ± 15.7	29.2 ± 21.0	38.6 ± 22.1